

cally, although it is favored thermodynamically. However, x-ray scanning reveals that the volume fraction in the fan above the sediment increases smoothly with depth, passing through the phase boundary at  $\phi = 0.50$  while the particles remained dispersed. For the 0.31- $\mu\text{m}$  particles at  $\phi \approx 0.53$ , the chemical potential of the disordered phase exceeds that of the ordered phase sufficiently to produce a crystallization rate equal to the kinematic velocity; hence, the transition produces a coexisting crystalline phase with  $\phi \approx 0.60$ . For the 0.43- $\mu\text{m}$  particles, the maximum crystallization rate apparently falls below the growth rate of an

amorphous sediment for the volume fractions reported here and crystallization does not occur. Thus, for these initial volume fractions there exists a maximum size above which particles settle too rapidly to find sites on a crystal lattice, resulting in amorphous sediments.

#### REFERENCES AND NOTES

1. L. V. Woodcock, *Ann. N.Y. Acad. Sci.* **37**, 274 (1981).
2. A. D. J. Haymet, *J. Chem. Phys.* **78**, 4641 (1983).
3. S. Hachisu and Y. Kobayashi, *J. Colloid Interface Sci.* **46**, 470 (1974).
4. P. N. Pusey and W. van Megen, *Nature* **320**, 340 (1986).
5. ———, *Phys. Rev. Lett.* **59**, 2083 (1987).
6. D. Frenkel and J. P. McTague, *Annu. Rev. Phys. Chem.* **31**, 491 (1980).
7. W. Stöber, A. Fink, E. Bohn, *J. Colloid Interface Sci.* **26**, 62 (1968).
8. A. K. van Helden *et al.*, *ibid.* **81**, 354 (1981).
9. C. G. de Kruif *et al.*, *J. Phys. (Paris)* **46**, 295 (1985).
10. P. Pieranski, *Contemp. Phys.* **24**, 25 (1983).
11. W. J. Glantschnig and A. Holliday, *Appl. Opt.* **26**, 983 (1987).
12. G. J. Kynch, *Trans. Faraday Soc.* **48**, 166 (1952).
13. K. E. Davis and W. B. Russel, *Adv. Ceramics* **21**, 573 (1987).
14. J. Q. Broughton *et al.*, *Phys. Rev. Lett.* **49**, 1496 (1982).
15. We are indebted to C. W. Draper for support of this research and to K. D. Pohl who handled much of the x-ray measurements. This work was performed under Department of Energy Office of Basic Energy Sciences grant DE-FG02-85ER45210.

6 March 1989; accepted 5 May 1989

## Hydrophobic Organization of Membrane Proteins

D. C. REES,\* L. DEANTONIO, D. EISENBERG

Membrane-exposed residues are more hydrophobic than buried interior residues in the transmembrane regions of the photosynthetic reaction center from *Rhodobacter sphaeroides*. This hydrophobic organization is opposite to that of water-soluble proteins. The relative polarities of interior and surface residues of membrane and water soluble proteins are not simply reversed, however. The hydrophobicities of interior residues of both membrane and water-soluble proteins are comparable, whereas the bilayer-exposed residues of membrane proteins are more hydrophobic than the interior residues, and the aqueous-exposed residues of water-soluble proteins are more hydrophilic than the interior residues. A method of sequence analysis is described, based on the periodicity of residue replacement in homologous sequences, that extends conclusions derived from the known atomic structure of the reaction center to the more extensive database of putative transmembrane helical sequences.

THREE-DIMENSIONAL PROTEIN structures reflect a favorable energetic balance between protein-protein and protein-solvent interactions. For water-soluble proteins, polar and charged residues are often on the surface, whereas apolar residues tend to occur in the interior (1-6). The hydrophobic organization of membrane proteins is less well understood, although models of membrane protein structures (7, 8) make use of the hydrophobic transmembrane  $\alpha$  helix and an "inside-out" pattern of residue hydrophobicity in which the interior residues are more polar than the membrane-exposed surface residues (9). The availability of atomic structures for bacterial photosynthetic reaction centers (RCs) (10-12) allows a more quantitative analysis of the hydrophobic organization of a membrane protein. The results of this analysis are

described for the RC from *Rhodobacter sphaeroides*. Based on these observations, a method of analysis of homologous sequences is proposed that may be generally useful in assigning interior and surface (membrane-exposed) residues of transmembrane helices from sequence information. Application of this method to a variety of membrane-protein families is described.

The RCs from purple bacteria consist of three membrane-bound subunits, containing a total of 11 transmembrane  $\alpha$  helices. The position in the membrane of the RC from *Rb. sphaeroides* was proposed (13) with the use of a hydrophobic free energy function (14) to establish the orientation of most favorable interaction between the RC and a nonaqueous phase. Amino acids located in the nonpolar region of the membrane were assigned (13) to one of three classes: buried, semi-exposed, and exposed residues, which were defined as having >80%, 50 to 80%, and <50%, respectively, of their accessible surface area in an isolated helix buried upon association of that helix in the RC structure. The average residue hydrophobicity in each class,  $\langle h \rangle$ , may be determined from the ami-

no acid composition of each class, combined with a measure of the hydrophobicity of each residue, from the relation:

$$\langle h \rangle = \sum c_i h_i \quad (1)$$

where  $c_i$  is the molar fraction of the  $i$ th amino acid in a particular class,  $h_i$  is the residue hydrophobicity, and the sum is over all 20 amino acids. Values for  $h_i$  are assigned from the consensus hydrophobicity scale of Eisenberg *et al.* (15). The average residue hydrophobicities for the buried, semi-exposed, and exposed classes are 0.19, 0.31, and 0.48, respectively (Table 1). Increasing apolarity is associated with more positive hydrophobicity values, so that buried residues in the membrane-spanning region of the RC are less hydrophobic than exposed residues. The greater hydrophobicity of exposed residues of the membrane-spanning helices in the RC structure is not sensitive to the precise definition of exposed and buried. Chothia (4) defined buried residues in water-soluble proteins as those having <5% of their surface accessible to solvent. With this criterion, average residue hydrophobicities

**Table 1.** Mean residue hydrophobicities for buried and exposed residues.

Protein types	Mean residue hydrophobicities	
	Buried	Exposed
<i>Transmembrane proteins</i>		
11 RC helices	0.19*	0.48
11 RC helices	0.22†	0.36
35 Helices (Table 2)	0.15‡	0.34
<i>Water-soluble proteins</i>		
37 Monomers	0.24†	-0.25
23 Oligomers	0.19†	-0.28
7 Hemoglobin helices	0.17‡	-0.26

Definition of buried residues: \* >80% area buried in helices (13); † <5% residue area exposed (4). ‡ Hydrophobic moment (25).

Department of Chemistry and Biochemistry, Molecular Biology Institute, University of California, Los Angeles, Los Angeles, CA 90024.

\*To whom correspondence should be sent at Division of Chemistry and Chemical Engineering 147-75 CH, California Institute of Technology, Pasadena, CA 91125.

for buried and surface residues in the transmembrane region of the RC from *Rb. sphaeroides* were 0.22 and 0.36, respectively (Table 1). Although the definition of buried and surface residues differs from that used above, consistent results for the relative hydrophobicities of these two classes are observed.

For purposes of comparison, the average hydrophobicities of buried and surface residues (as defined by the 5% surface area criterion) in water-soluble proteins of known structure were determined from values of  $c_i$  tabulated in (6) for 37 monomeric and 23 oligomeric water-soluble proteins. The average residue hydrophobicities (Eq. 1) for buried residues were 0.24 and 0.19 and for surface residues were  $-0.25$  and  $-0.28$ , for monomeric and oligomeric water-soluble proteins, respectively (Table 1). Comparison of these values to those determined for the RC reveals that the average residue hydrophobicities for buried residues are nearly identical for the two classes of proteins. In contrast, the surface residues of water-soluble proteins are more polar than the interior, whereas the surface residues in the RC are more apolar than the interior. The gradient of hydrophobicity between buried and surface residues is opposite for water-soluble and membrane proteins. There is not, however, a simple reversal of polarity for buried and surface residues in that the interior regions of both classes of proteins exhibit comparable hydrophobicities.

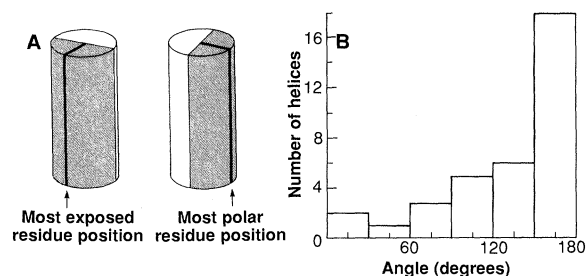
Since the database for membrane proteins

**Table 2.** Membrane-protein families used in the sequence analysis described in the text. Sequence alignments and identification of potential transmembrane helices were based on assignments proposed in the references. Residue boundaries for a representative sequence of each helix are presented in Table 3. Some adjustments were made with the programs BESTFIT and PROFMAKE (22) for consistency in alignment over an entire sequence family.

Family	Number of transmembrane helices	Number of sequences
Reaction center (16)	5	10*
Bacteriorhodopsin (17)	7	2
G-protein-linked receptors (18)	7	28
Na, Ca ion channels (19)	6	20†
Cytochrome bc <sub>1</sub> /b <sub>6</sub> f (20)	8	18
Sensory transducers (21)	2	4

\*Includes five sequences each from the two homologous (L and M) subunits of bacterial RCs. †Includes five sequences each with four internal repeats.

**Fig. 1.** (A) Cylindrical model for helical sequence analyses described in the text. Helical properties (such as residue polarity and solvent exposure) are assumed to be a function only of the rotation angle about the helical axis and not of the position along the helix axis. (B) Histogram of the angle between variable and hydrophilic sides of 35 transmembrane helical sequences of Table 2.



contains only one family of three-dimensional structures (RCs), it is desirable to extend this analysis to include extensive sequence information available for a larger set of membrane proteins. Locations of transmembrane-spanning  $\alpha$  helices in sequences of homologous proteins have been tentatively assigned by others from hydrophobicity analyses (7). Estimates of the exposed and hydrophilic surfaces of these putative helices may be determined from sequence information, as described below. Comparison of the relative positions of the exposed and hydrophilic helical surfaces may then be used to address the generality of the hydrophobic organization observed in the RC structure.

The exposed and hydrophilic surfaces of 35 potential transmembrane helices from six membrane protein families were determined as follows. Sequence alignments of the families were obtained from the literature (Table 2) (16–22). Positions in these sequences of the most exposed and most polar residues were assigned by two related methods. For both calculations, a simple model treating the assumed  $\alpha$  helix conformation as a cylinder was used (Fig. 1A). Lines running parallel to the helix axis representing the positions of greatest residue exposure or polarity are identified from sequence information, and may be used to divide each cylinder into two regions of equal area for classification purposes. This model for dividing up every helix surface into exposed or polar regions is simplistic; in the absence of structural information, however, a more detailed model would not be justified.

Membrane-exposed residues in the transmembrane helices of the RC are less well conserved among homologous proteins than the interior residues (13). Surface residues are more variable than buried residues in water-soluble proteins as well (23). Fourier methods (16, 24) can be used to assess periodicity in the pattern of residue conservation in a family of protein sequences. A variability profile,  $V$ , is constructed for a particular family of sequences. The  $V_j$  element of this profile is defined by the number of different types of amino acid residues that are observed at a given position  $j$  in a family of aligned sequences. The periodic compo-

nent of  $V$  that reflects the (assumed)  $\alpha$ -helical conformation of these sequences may be described by the Fourier terms:

$$A(\omega) = \sum_{j=1}^N (V_j - \langle V \rangle) \cos(j\omega)$$

$$B(\omega) = \sum_{j=1}^N (V_j - \langle V \rangle) \sin(j\omega) \quad (2)$$

where  $N$  is the number of residues in the sequence,  $\langle V \rangle$  is the average value of  $V$  for the sequence, and  $\omega$  is the angular rotation angle (in radians) between residues around the helical axis (it equals  $5\pi/9$  radians or  $100^\circ$  for an ideal helix). The most variable stripe running parallel to the helix axis occurs at sequence positions where the Fourier component with  $\omega = 100^\circ$  is maximal, which occurs for residue positions  $f$  (which may be noninteger in this situation) that satisfy the relation:

$$f = (3.6/2\pi) \tan^{-1}[B(\omega)/A(\omega)] + 3.6n \quad (3)$$

where  $n$  is an integer and  $A$  and  $B$  are given by Eq. 2 with  $\omega = 100^\circ$ . The strength of the  $\alpha$ -helical periodicity in the substitution profile may be characterized by the parameter  $\psi$ ;  $\psi > \sim 1.5$  indicates a surface-bound helix (16, 24), whereas  $\psi < \sim 1$  indicates helices that are either buried inside the protein or are completely surrounded by lipid. In Table 3,  $\psi$  values and the most variable positions in a representative sequence for each of the 35 transmembrane helices are listed. In view of the correlation between variable and exposed residues in the RC structure, we assume that these positions define the membrane-exposed side of a helix.

The most hydrophobic side in a transmembrane helix may be determined by replacing the  $V_j$  in Eq. 2 with the average residue hydrophobicity for all the residues observed at a position  $j$ . This calculation is equivalent to determining the orientation of the hydrophobic moment (25) about the helix axis. The amphiphilic index  $H$  (26), which is analogous to  $\psi$ , characterizes the strength of the helical periodicity in the hydrophobicity pattern. The hydrophilic positions are displaced from the hydrophobic positions by half the helical repeat, or 1.8 residues (see Table 3).

If the hydrophobic organization of the RC structure—the more hydrophilic helical surface being opposite the more exposed surface—is general in membrane proteins, then the same result should be found for other transmembrane helices. The relative orientations of the exposed and hydrophilic surfaces about the helical axis are determined from the absolute difference between

the most variable and most hydrophilic residue positions. This difference can be converted to an angular rotation about the helix axis (multiplying by  $\omega = 100^\circ$ ), yielding the histogram in Fig. 1B for the 35-transmembrane helices listed in Tables 2 and 3. The exposed and hydrophilic surfaces tend to be on opposite sides of membrane-spanning helices. The average angle between the ex-

posed and hydrophilic position is  $129^\circ$ . For a similar calculation with seven aligned helices in hemoglobin [(27), Table 3], the average angle between variable and hydrophilic helical positions is  $31^\circ$ . The results of this sequence analysis are consistent with observations on the hydrophobic organization of the RC structure and support the idea that the relative polarity of the surface and interior residues are reversed between membrane proteins and water-soluble proteins.

Average residue hydrophobicities for the surface and interior regions of transmembrane helices may also be derived from sequence alignments by using the correlation that surface residues constitute the more hydrophobic helical face, whereas buried residues constitute the more polar helical face. Amino acids within 1/4 helical turn (0.9 residues) of the most hydrophilic positions are classified as interior residues (for membrane proteins), whereas the remaining positions are classified as surface residues (Fig. 1A). The resulting amino acid compositions may be used in Eq. 1 to determine average residue hydrophobicities of 0.34 and 0.15 for the surface and interior helical faces, respectively (Tables 1 and 3), of the transmembrane sequences in Table 2. A similar analysis of  $\alpha$  helices in hemoglobin yields average residue hydrophobicities for the surface and interior faces of  $-0.26$  and  $0.17$ , respectively (Tables 1 and 3). These analyses of helical sequences support the observations from the *Rb. sphaeroides* RC structure that the average hydrophobicity of interior facing residues is comparable for both water-soluble and membrane proteins. This general trend does not, however, exclude the presence of helices in the transmembrane region with polar groups having specific structural or functional purposes; the S4 helix of the Na,Ca ion channel (Table 3) may represent one such example.

Previously, similarities in such structural features as surface area and atomic packing between the RC and water-soluble proteins have been described (13). The equivalence of residue hydrophobicity in the interiors of water-soluble and membrane proteins further supports a unifying view of protein structure in which the structural organization of water-soluble and membrane proteins reflect variations on the same themes (24). In particular, membrane and water-soluble proteins exhibit comparable interior characteristics and differ primarily in the chemical polarity of the surface residues that serve to solubilize these proteins in the appropriate environment. An implication of this view is that van der Waals forces among the many atoms in the close-packed interiors of both membrane and water-soluble proteins are crucial for protein stability.

**Table 3.** Characterization of the variability and hydrophobicity properties of representative sequences from 35 transmembrane helical segments.  $\psi$  and  $H$  characterize the helical periodicity of the variability and hydrophobicity profiles, respectively, of these segments;  $HL$  and  $HB$  are the average hydrophobicities of residues assigned to the hydrophilic and hydrophobic surfaces, respectively, of the sequences (see text). Hemoglobin helices are included as representative water-soluble protein sequences. Additional “most variable” and “most hydrophilic” positions (in residue number) may be generated by the addition of integer multiples of 3.6 residues (the helix repeat) to the positions listed in the table.

Helix (residues)*	Variability	Hydrophobicity			Most variable positions	Most hydrophilic positions
	$\psi$	$H$	$HL$	$HB$		
			<i>Reaction center</i>			
A(54–74)	2.3	1.4	0.27	0.40	57.3,60.9,...	55.4,59.0,...
B(113–133)	2.7	1.4	0.14	0.23	116.2,119.8,...	114.3,117.9,...
C(147–166)	3.2	1.4	0.13	0.39	148.0,151.6,...	149.7,153.3,...
D(200–218)	1.3	0.3	0.23	0.26	200.5,204.1,...	201.6,205.2,...
E(268–286)	1.2	1.4	0.23	0.44	270.6,274.2,...	269.0,272.6,...
			<i>Bacteriorhodopsin</i>			
A(8–31)	0.9	0.9	0.19	0.34	8.1,11.7,...	8.8,12.4,...
B(41–64)	1.4	1.7	0.20	0.28	41.0,44.6,...	44.4,48.0,...
C(79–101)	1.1	1.6	-0.07	0.34	81.1,84.7,...	82.0,85.6,...
D(107–130)	1.2	1.3	0.06	0.38	109.1,112.7,...	107.1,110.7,...
E(133–156)	0.8	1.1	0.11	0.36	136.1,139.7,...	134.0,137.6,...
F(175–198)	2.4	1.2	0.05	0.33	176.1,179.7,...	175.0,178.6,...
G(202–225)	1.3	1.1	0.00	0.27	202.8,206.4,...	204.8,208.4,...
			<i>G protein-linked receptors</i>			
1(39–61)	2.4	1.5	0.25	0.40	42.1,45.7,...	40.5,44.1,...
2(74–96)	0.8	0.4	0.24	0.23	77.5,81.1,...	75.9,79.5,...
3(112–136)	2.2	0.8	-0.03	0.26	115.1,118.7,...	113.3,116.9,...
4(153–173)	3.3	1.8	0.20	0.39	155.0,158.6,...	153.3,156.9,...
5(203–227)	2.4	0.7	0.21	0.35	206.2,209.8,...	203.5,207.1,...
6(253–276)	1.6	1.3	0.22	0.37	255.0,258.6,...	253.4,257.0,...
7(286–309)	1.5	2.9	-0.02	0.28	289.5,293.1,...	288.2,291.8,...
			<i>Na,Ca channels</i>			
S1(124–147)	1.2	0.5	0.12	0.35	126.1,129.7,...	124.3,127.9,...
S2(156–175)	2.9	2.0	0.02	0.32	159.3,162.9,...	157.9,161.5,...
S3(189–207)	2.9	1.6	0.08	0.39	192.1,195.7,...	190.5,194.1,...
S4(214–233)	1.7	3.4	-0.17	-0.12	216.7,220.3,...	214.7,218.3,...
S5(250–271)	1.5	1.2	0.36	0.35	251.2,254.8,...	252.7,256.3,...
S6(401–424)	0.8	0.6	0.29	0.48	401.2,404.8,...	403.0,406.6,...
			<i>Cytochrome bc<sub>1</sub>/b<sub>6</sub>f</i>			
1(35–56)	4.9	1.6	0.14	0.34	35.3,38.9,...	36.7,40.3,...
2(80–100)	0.7	1.1	-0.13	0.18	81.6,85.2,...	82.8,86.4,...
3(112–133)	1.8	0.9	0.28	0.41	114.3,117.9,...	112.3,115.9,...
4(149–160)	2.4	3.3	-0.05	0.43	150.9,154.5,...	151.0,154.6,...
5(168–190)	1.1	1.1	0.26	0.41	170.7,173.3,...	169.4,gap
6(219–240)	1.2	0.8	0.32	0.39	220.8,224.4,...	220.0,223.6,...
7(278–297)	2.3	2.3	0.30	0.49	278.7,282.3,...	279.7,283.3,...
8(310–328)	1.5	0.6	0.18	0.37	313.2,316.8,...	311.9,315.5,...
			<i>Sensory transducers</i>			
1(17–43)	1.7	1.6	0.26	0.35	19.1,22.7,...	18.8,22.4,...
2(198–221)	0.7	0.5	0.35	0.42	201.4,205.0,...	198.5,202.1,...
			<i>Hemoglobin</i>			
A(3–17)	1.3	1.1	-0.25	0.03	4.6,8.2,...	4.5,8.1,...
B(24–35)	1.1	2.4	-0.26	0.33	27.1,30.7,...	27.1,30.7,...
C(36–43)	0.6	1.6	-0.30	0.18	38.3,41.9,...	37.3,40.9,...
E(52–72)	2.9	2.4	-0.32	0.16	53.1,56.7,...	53.4,57.0,...
F(80–89)	3.1	2.0	-0.27	0.15	81.7,85.3,...	81.5,85.1,...
G(94–112)	1.9	1.1	-0.16	0.09	96.2,99.8,...	95.9,99.5,...
H(122–138)	1.4	2.9	-0.23	0.25	122.7,126.3,...	123.0,126.6,...

\*Representative sequences: *Rb. sphaeroides* M subunit; *H. halobium* bacteriorhodopsin; bovine rhodopsin; rat Na channel III domain I; human cytochrome bc<sub>1</sub>/b<sub>6</sub>f; Trg; and human  $\alpha$  chain.

## REFERENCES AND NOTES

- W. Kauzmann, *Adv. Protein Chem.* **14**, 1 (1959).
- M. F. Perutz, J. C. Kendrew, H. C. Watson, *J. Mol. Biol.* **13**, 669 (1965).
- B. Lee and F. M. Richards, *ibid.* **55**, 379 (1971).
- C. Chothia, *ibid.* **105**, 1 (1976).
- G. D. Rose *et al.*, *Science* **229**, 834 (1985).
- S. Miller *et al.*, *J. Mol. Biol.* **196**, 641 (1987); J. Janin, S. Miller, C. Chothia, *ibid.* **204**, 155 (1988).
- J. Kyte and R. F. Doolittle, *ibid.* **157**, 105 (1982).
- D. Eisenberg, *Annu. Rev. Biochem.* **53**, 595 (1984); D. M. Engleman, T. A. Steitz, A. Goldman, *Annu. Rev. Biophys. Biophys. Chem.* **15**, 321 (1986).
- D. M. Engelman and G. Zaccari, *Proc. Natl. Acad. Sci. U.S.A.* **77**, 5894 (1980).
- J. Deisenhofer *et al.*, *J. Mol. Biol.* **180**, 385 (1984); *Nature* **318**, 618 (1985).
- J. P. Allen *et al.*, *Proc. Natl. Acad. Sci. U.S.A.* **83**, 8589 (1986); J. P. Allen, G. Feher, T. O. Yeates, H. Komiya, D. C. Rees, *ibid.* **84**, 5730 (1987).
- C.-H. Chang *et al.*, *FEBS Lett.* **205**, 82 (1986).
- T. O. Yeates *et al.*, *Proc. Natl. Acad. Sci. U.S.A.* **84**, 6438 (1987).
- D. Eisenberg and A. D. McLachlan, *Nature* **319**, 199 (1986).
- D. Eisenberg, R. M. Weiss, T. C. Terwilliger, W. Wilcox, *Faraday Symp. Chem. Soc.* **17**, 109 (1982); Hydrophobicities are: Ala, 0.25; Arg, -1.76; Asn, -0.64; Asp, -0.72; Cys, 0.04; Glu, -0.62; Gln, -0.69; Gly, 0.16; His, -0.40; Ile, 0.73; Leu, 0.53; Lys, -1.10; Met, 0.26; Phe, 0.61; Pro, -0.07; Ser, -0.26; Thr, -0.18; Trp, 0.37; Tyr, 0.02; and Val, 0.54.
- H. Komiya *et al.*, *Proc. Natl. Acad. Sci. U.S.A.* **85**, 9012 (1988).
- H. G. Khorana, *J. Biol. Chem.* **263**, 7439 (1988); A. Blanck and D. Oesterhelt, *EMBO J.* **6**, 265 (1987).
- J. Nathans and D. S. Hogness, *Cell* **34**, 807 (1983); A. F. Cowman, C. S. Zuker, G. M. Rubin, *ibid.* **44**, 705 (1986); D. Young, G. Waitsches, C. Birchmeier, O. Fasano, M. Wigler, *ibid.* **45**, 711 (1986); J. Nathans, D. Thomas, D. S. Hogness, *Science* **232**, 193 (1986); B. K. Kobilka *et al.*, *ibid.* **238**, 650 (1987); T. I. Bonner, N. J. Buckley, A. C. Young, M. R. Brann, *ibid.* **237**, 527 (1987); D. Julius, A. B. MacDermott, R. Axel, T. M. Jessell, *ibid.* **241**, 558 (1988); J. Nathans and D. S. Hogness, *Proc. Natl. Acad. Sci. U.S.A.* **81**, 4851 (1984); Y. Yarden *et al.*, *ibid.* **83**, 6795 (1986); T. Frielle *et al.*, *ibid.* **84**, 7920 (1987); J. Gocayne *et al.*, *ibid.*, p. 8296; K. J. Fryxell and E. M. Meyerowitz, *EMBO J.* **6**, 443 (1987); E. G. Peralta *et al.*, *ibid.*, p. 3923; R. A. F. Dixon *et al.*, *Nature* **321**, 75 (1986); T. Kubo *et al.*, *ibid.* **323**, 411 (1986); Y. Masu *et al.*, *ibid.* **329**, 836 (1987); P. R. Schofield, L. M. Rhee, E. G. Peralta, *Nucleic Acids Res.* **15**, 3636 (1987); T. Kubo *et al.*, *FEBS Lett.* **209**, 367 (1986).
- T. Kayano, M. Noda, V. Flockner, H. Takahashi, S. Numa, *FEBS Lett.* **228**, 187 (1988); T. Tanabe *et al.*, *Nature* **328**, 313 (1987).
- G. Hauska, W. Nitschke, R. G. Herrmann, *J. Bioenerg. Biomembr.* **20**, 211 (1988).
- J. L. Bollinger *et al.*, *Proc. Natl. Acad. Sci. U.S.A.* **81**, 3287 (1984); A. Krikos, N. Mutoh, A. Boyd, M. I. Simon, *Cell* **33**, 615 (1983).
- J. Devereux, P. Haerberli, O. Smithies, *Nucleic Acid Res.* **12**, 387 (1984); M. Gribskov, A. D. McLachlan, D. Eisenberg, *Proc. Natl. Acad. Sci. U.S.A.* **84**, 4355 (1987).
- E. L. Smith, *Harvey Lect.* **62**, 231 (1967); C. Chothia and A. M. Lesk, *EMBO J.* **5**, 823 (1986); J. F. Reidhaar-Olson and R. T. Sauer, *Science* **241**, 53 (1988).
- D. C. Rees, H. Komiya, T. O. Yeates, J. P. Allen, G. Feher, *Annu. Rev. Biochem.* **58**, 607 (1989).
- D. Eisenberg, R. M. Weiss, T. C. Terwilliger, *Proc. Natl. Acad. Sci. U.S.A.* **81**, 140 (1984).
- J. L. Cornette *et al.*, *J. Mol. Biol.* **195**, 659 (1987).
- A. M. Lesk and C. Chothia, *ibid.* **136**, 225 (1980).
- We thank J. P. Allen and G. Feher for helpful discussions. Supported by NIH grants GM31299 and GM39558. D.C.R. is an A. P. Sloan research fellow. Programs and sequence alignments used in this work are available from D.C.R.

3 March 1989, accepted 2 June 1989

## Interpretation of Cloud-Climate Feedback as Produced by 14 Atmospheric General Circulation Models

R. D. CESS, G. L. POTTER, J. P. BLANCHET, G. J. BOER, S. J. GHAN, J. T. KIEHL, H. LE TREUT, Z.-X. LI, X.-Z. LIANG, J. F. B. MITCHELL, J.-J. MORCRETTE, D. A. RANDALL, M. R. RICHES, E. ROECKNER, U. SCHLESE, A. SLINGO, K. E. TAYLOR, W. M. WASHINGTON, R. T. WETHERALD, I. YAGAI

**Understanding the cause of differences among general circulation model projections of carbon dioxide-induced climatic change is a necessary step toward improving the models. An intercomparison of 14 atmospheric general circulation models, for which sea surface temperature perturbations were used as a surrogate climate change, showed that there was a roughly threefold variation in global climate sensitivity. Most of this variation is attributable to differences in the models' depictions of cloud-climate feedback, a result that emphasizes the need for improvements in the treatment of clouds in these models if they are ultimately to be used as climatic predictors.**

OBSERVED AND PROJECTED INCREASES in the concentration of atmospheric CO<sub>2</sub> and other greenhouse gases have stimulated considerable interest in modeling climatic change. The most detailed climate models for this purpose are three-dimensional general circulation models (GCMs). Although most GCMs are of similar design, there are significant differences among GCM projections of climatic warming as induced by increasing levels of atmospheric carbon dioxide (1, 2). The reasons for these differences are not fully understood, but variations in how cloud-climate feedback processes are simulated in the various models are thought to be largely responsible (3); cloud feedback is dependent on all aspects of a model and not just on cloud formation parameterizations. Clearly there is a need to isolate and to understand better cloud feedback mechanisms in GCMs, and, more specifically, to determine if they are a significant cause of intermodel differences in recent climate-change projections. Consequently we have made an intercomparison of cloud feedback in 14 atmospheric GCMs as part of a larger study directed toward improving GCMs and climatic projections.

Many facets of the climate system are not well understood, and thus the uncertainties in modeling atmospheric, cryospheric, and oceanic interactions are large. In evaluating the differences among models, we have focused first on atmospheric processes, because these uncertainties must be understood before others can be addressed. For simplicity, we have emphasized solely global-average quantities, and we adopted the conventional interpretation of climate change as a two-stage process: forcing and response (4). The concept of global-average forcing and response has proven useful in earlier interpretations of cloud-climate feedback. For example, by performing two

GCM simulations for a doubling of atmospheric CO<sub>2</sub> concentration, one with computed clouds and the other with clouds that were invariant to the change in climate, Wetherald and Manabe have suggested (5) that cloud-climate feedback amplifies global warming by the factor 1.3. A somewhat larger amplification (1.8) was estimated by Hansen *et al.* (6) using a one-dimensional climate model to evaluate climate feedback mechanisms in a different GCM.

The global-mean direct radiative forcing,  $G$ , of the surface-atmosphere system is evaluated by holding all other climate parameters fixed. It is this quantity that induces the ensuing climate change, and physically it represents a change in the net (solar plus infrared) radiative flux at the top of the atmosphere (TOA). For an increase in the CO<sub>2</sub> concentration of the atmosphere,  $G$  is the reduction in the emitted TOA infrared flux resulting solely from the CO<sub>2</sub> increase, and this reduction results in a heating of the surface-atmosphere system. The response

R. D. Cess, Institute for Atmospheric Sciences, State University of New York, Stony Brook, NY 11794.  
G. L. Potter, S. J. Ghan, K. E. Taylor, Lawrence Livermore National Laboratory, Livermore, CA 94550.  
J. P. Blanchet and G. J. Boer, Canadian Climate Centre, Downsview, Ontario M3H 574, Canada.  
J. T. Kiehl, A. Slingo, W. M. Washington, National Center for Atmospheric Research, Boulder, CO 80307.  
H. Le Treut and Z.-X. Li, Laboratoire de Météorologie Dynamique, 24 Rue Lhomond, 75231 Paris Cédex 05, France.  
X.-Z. Liang, Institute of Atmospheric Physics, Beijing, China.  
J. F. B. Mitchell, United Kingdom Meteorological Office, Bracknell, Berkshire RG12 25, England.  
J.-J. Morcrette, European Centre for Medium-Range Weather Forecasts, Reading, Berkshire RG2 9AX, England.  
D. A. Randall, Colorado State University, Fort Collins, CO 80523.  
M. R. Riches, Department of Energy, Washington, DC 20545.  
E. Roeckner and U. Schlese, University of Hamburg, Bundesstrasse 55, D2000, Hamburg 13, Federal Republic of Germany.  
R. T. Wetherald, Geophysical Fluid Dynamics Laboratory, Princeton University, Princeton, NJ 08540.  
I. Yagai, Meteorological Research Institute of Japan, Ibaraki-Ken, 305 Japan.